**Research Article**

# Lithium-containing radiator materials for neutron ionization chambers[*]

Petr B. Baskov[1], Boris S. Salamakha[1], Yakov V. Glazyuk[1], Artur A. Namakshinas[1],
Sergey A. Bondarenko[1], Ilya M. Mushin[1], Alexander S. Khudin[1]

1 *NIKIET JSC, 1 Acad.Dollezhal Sq., bldg. 3, 107140 Moscow, Russia*

Corresponding author: Artur A. Namakshinas (namakshinas_aa@nikiet.ru)

**Citation:** Baskov PB, Salamakha BS, Glazyuk YV, Namakshinas AA, Bondarenko SA, Mushin IM, Khudin AS (2025) Lithium-containing radiator materials for neutron ionization chambers. Nuclear Energy and Technology 11(1): 65–70. https://doi.org/10.3897/nucet.11.151566

## Abstract

The paper presents the results of material testing for the purpose of obtaining radiator material – acomposite coating with neutron conversion material – for ionization chambers (IC) which contain the $^6$Li isotope and convert neutron radiation to a flux of high-energy charged particles through the $^6$Li(n, α)$^3$H nuclear reaction. The proposed method for forming lithium-containing radiator material allows ensuring a high temperature resistance of up to 600 °C and a mechanical strength at the expense of adhesion to the IC electrode material (grade 321 steel). The advantages of a lithium-containing radiator, compared to a boron radiator, are explained by the smaller cross-section of the $^6$Li-neutron interaction: the smaller efficiency of the "neutron → charged particle" conversion is made up for by a high power density and a prolonged free path of reaction products in the radiator material, which makes it possible to increase the surface density of $^6$Li atoms, while reducing the extent of "burnup" in neutron fields. The IC electrode radiator material consists of a two-layer composite coating comprising an adhesive silicate layer and a functional neutron-sensitive lithium fluoride layer. Measurements at an alpha spectrometric facility have shown that the coating has a high energy output (~ $2.8 \cdot 10^{-3}$ MeV/neutron), which remains stable after four thermal cycles of up to 600 °C. The coating is resistant to vibration when exposed to frequencies of 35 to 200 Hz. The paper presents the results of testing the IC mockup with a lithium-containing radiator material. When irradiated with a neutron flux of $6 \cdot 10^3$ cm$^{-2}$·s$^{-1}$, the IC mockup sensitivity value was about $10^{-15}$A·s·cm$^2$/neutron, which agrees with the calculated value.

## Keywords

neutron detectors, ionization chamber, radiator material, functional neutron-sensitive lithium fluoride layer

## Introduction

Ionization fission chambers with radiator coatings based on isotopes,such as $^{235}$U, $^{238}$U and $^{232}$Th, and boron ionization chambers (with the$^{10}$B isotope used as the radiator), the technology of which was developed in the past century, are currently employed for neutron diagnostics at nuclear power plants.

The need for developing new neutron detectors is dictated by the change in operating conditions of radiation devices. Temperatures of up to 600 °C, neutron fluxes of up to $1 \cdot 10^{17}$ cm$^{-2}$·s$^{-1}$, and vibration loads of up to 200 Hz are reached in the present-day reactor cores (Baskov et al. 2022). Expanding the temperature range of ionization fission chambers, based on the electrical principle

---

\* Russian text published: Izvestiya vuzov. Yadernaya Energetika (ISSN 0204-3327), 2024, n. 4, pp. 56–68.

of operation, by organizing heterostructured nano-level uranium-oxide radiator coatings with a surface density of 1.2 mg/cm$^2$ is proposed in (Sakharov et al. 2012a, 2012b; Egorov et al. 2015; Glazyuk et al. 2017; Baskov et al. 2018) to support neutron diagnostics of current reactor plants.

There is no information in open sources on materials based on the $^6$Li isotope used as the IC radiator coatings. The key types of neutron detecting lithium-containing materials are lithium-silicate glass (Voytovetsky and Tolmacheva 1959, 1961; Shulgin et al. 2005) and crystal scintillators with the ZnS(Ag)/$^6$LiF composition (Osovizky et al. 2018; Mosset et al. 2014). The use of the $^6$Li isotope and its compounds as the IC radiator materials is limited by their high reactivity and volatility (Allen 1962; Subbotin et al. 1999).

Using the $^6$Li isotope is promising in terms of forming radiator coatings which will feature a smaller "burnup" as compared with existing boron ($^{10}$B isotope) radiator coatings. The balance of the number of active radiator nuclei is determined by equation (Dmitriev, Malyshev 1975):

$$\frac{dN}{dt} = -\Phi \cdot \sigma \cdot N \qquad (1)$$

where $\Phi$ is the neutron flux; $\sigma$ is the cross-section of interaction with the neutron; $N$ is the number of active radiator nuclei; and $t$ is time.

It follows from equation (1) that the larger is the cross-section, the larger is the radiator material "burnup". The $^6$Li (n,α)$^3$H nuclear reaction cross-section (940 barns) is four times as small as for the $^{10}$B(n,α)$^7$Li reaction (3840 barns). At the same time, the power density of the $^6$Li(n, α)$^3$H reaction (4.80 MeV) is 1.7 times as high as in the event of $^{10}$B(n,α)$^7$Li reaction (2.79 MeV), and the path length of the $^6$Li(n,α)$^3$H reaction products is larger than that for the $^{10}$B(n,α)$^7$Li. This makes it possible to reduce the "burnup" of the lithium-containing layer and increase its efficiency. A higher energy yield creates conditions for using ICs based on the $^6$Li isotope both in the current and pulsed neutron recording modes. The development of the electronic component base and computer equipment allows nowadays to record individual fission events, which is expected to replace the classic actinide-based fission chambers.

# Formation of lithium-containing radiator coatings for IC electrodes

The method proposed to obtain the IC lithium-containing radiator coatings is formation of a composite two-layer coating. The adhesion of the functional neutron-sensitive lithium-containing layer to the surface of the grade 321 steel (IC electrode material) will be achieved using an "adhesive" intermediate silicate layer.

Lithium fluoride, the most chemically and thermally stable compound (melting point of 848 °C), has been chosen as the functional base for the lithium-containing radiator coating.

Fluoride-ion, as a ligand, has a relatively small atomic weight (19 g/mole), which will allow as many target atoms of the $^6$Li isotope as possible to be formed on the surface. It needs to be taken into account that the thickness of the formed functional lithium-containing layer of the composite coating requires to be proportional to the path lengths of the alpha particle and tritium in the lithium fluoride environment, which is determined by the Bragg equation (Bolozdynya 2017)

$$\frac{R_1}{R_0} = \frac{\rho_0 \sqrt{A_1}}{\rho_1 \sqrt{A_0}} \qquad (2)$$

where $R_0$ is the path length of the alpha particle (tritium) in air; $R_1$ is the path length of the alpha particle (tritium) in the environment; $\rho_0$ is the density of air; $\rho_1$ is the density of the environment; $A_0$ is the molar mass of air; and $A_1$ is the molar mass of the environment.

The path lengths of the alpha particle ($R_0 = 4.5$ μm) and tritium ($R_0 = 26.1$ μm) were determined from the nomograms of the path length and energy ratio (Experimental nuclear physics. Volume 1. 1955).

The material of the intermediate silicate layer in a plastic state is mechanically applied to the electrode surface, the surface roughness parameters of which are $Ra = 5.3$ μm and $Rz = 29.2$ μm. The material of the intermediate silicate layer penetrates into the microscopic dimpleson the electrode surface and is retained in these mechanically. Thixotropically, the solidifying silicate base also has a developed surface with parameters $Ra = 12.3$ μm and $Rz = 23.9$ μm. This promotes the adhesion of the deposited finely-dispersed lithium fluoride powder to the surface of the intermediate silicate layer while the latter is in a plastic state. In the process of drying, a composite two-layer coating with a lithium fluoride layer surface density of 2.5 mg/cm$^2$ is finally formed.

The microstructure of the composite radiator coating sample is shown in Fig. 1. A lithium fluoride layer with a thickness of 10 to 20 μm is applied to the surface of the intermediate silicate layer with a thickness of about 150 to 170 μm.

It was found by the X-ray phase analysis (XRD) (Papko, Kravchuk 2013) that the silicate base of the intermediate coating layer consists predominantly of alph-aquartz. Additional infrared spectroscopy investigations (Fig. 2) show that the silicate base includes a clay mineral (kaolinite). A broad band with 1098 cm$^{-1}$ is caused by the valence vibrations of the silicon-oxygen backbone tetrahedrons, and the narrow absorption bands with 798, 779 and 695 cm$^{-1}$ belong to alpha quartz. The bands in the region with 515 and 463 cm$^{-1}$ belong to the deformation oscillations of the alpha quartz silicon-oxygen groups (Plyusnina 1977). The narrow absorption lines with maximums at 3704 and 3620 cm$^{-1}$ coincide with the analytical absorption lines of the valence vibrations of the kaolinite hydroxyl groups (Nakamoto 1966). Following the heat treatmentat 600 °C, the disappearance of these absorption bands in the sample's infrared spectrum is observed, which is associated with the kaolinite
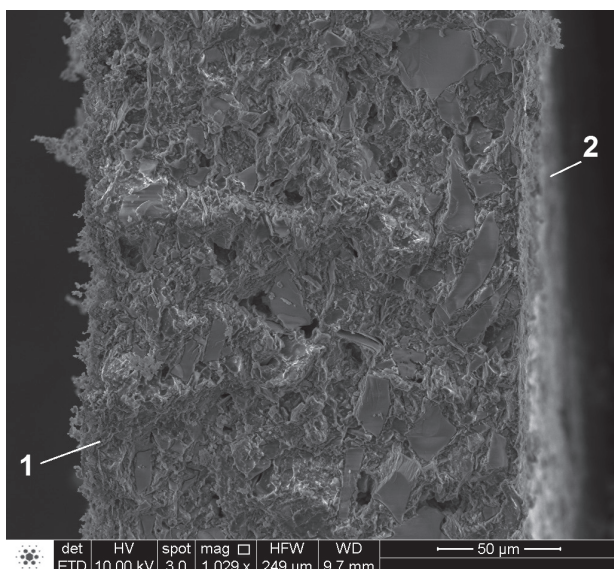
**Figure 1.** Microstructure (cross-sectional view) of a composite two-layer coating: 1 – intermediatesilicate layer; 2 – functional lithium fluoride layer.



**Figure 2.** Infrared absorption spectra of the composite coating intermediate layer silicate base: 1 – prior to heat treatment; 2 – afterheat treatment at 600 °C.

dehydration. The texture of the radiator coating intermediate layer (see Fig. 1) consists of alphaquartz grains (up to 30 μm), which are bound by the kaolinite veins.

It was shown by investigating the thermal action effect on the radiator coating material structure using the XRD method that, following a heat treatment at 600 °C, the materials of the intermediate silicate layer (alphaquartz, kaolinite) and the functional (lithium fluoride) layers of the radiator coating did not chemically interact with each other, since the diffraction patterns for the mixture of these substances is a superposition of the alphaquartz and lithium fluoride diffraction patterns (Fig. 3).

# Testing of lithium-containing radiator coatings for vibration stability

Lithium-containing radiator coatings were tested for resistance to mechanical overloads in horizontal and vertical planes under the action of vibrations at the VEDS-1500 vibration test bench. The samples were sequentially exposed to high frequency (200 Hz) vibrations with different acceleration amplitudes (1 to 8 $g$), the exposure time for each of the modes having been 30 min. It was found that the surface density of the composite radiator coating functional layer of 2.5 mg/cm$^2$ does not vary and, therefore, the coating remains intact. Composite coatings were also tested under the action of low-frequency resonant vibrations in accordance with GOST 29075-91 (GOST 29075-91, 2004). Test conditions: frequency intervals 6–8, 8–10, 10–13, 13–16, 16–20, 20–26, 26–35 Hz, acceleration amplitude 1.5 $g$, vibration exposure time for each frequency interval 15 min. Vibrations were changed from a lower frequency to an upper frequency with exposure at the highest upper
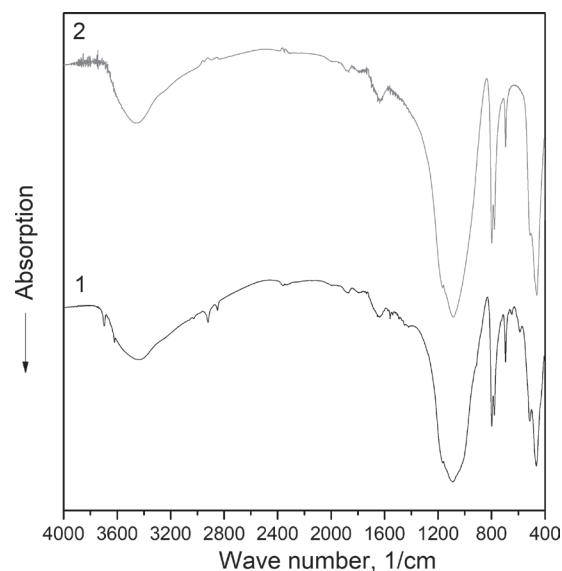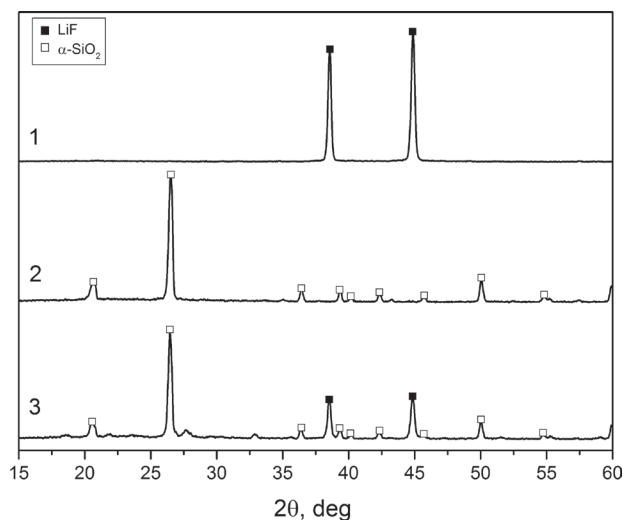


**Figure 3.** Diffraction patterns of the radiator coating components: 1 – lithium fluoride after heat treatment at 600°C, 2 – silicate base after heat treatment at 600°C, 3 – mixture of lithium fluoride and silicate base (ratio 1:2) after heat treatment at 600 °C.

frequency of each interval. The surface density of the functional layer prior to and after the tests remained unchanged and was 2.5 mg/cm$^2$. The results of the vibration resistance tests evidence that the lithium-containing radiator coating has high adhesive properties.

# Radiometric characteristics of lithium-containing radiator coatings for IC electrodes

Radiometric testing of electrode samples with a lithium-containing radiator coating were undertaken at an experimental test bench under the action of the neutron flux of 104 cm

$^2 \cdot$s$^{-1}$ from a Pu-Be source. The energy yield from the radiator coating surface is determined from the spectrum obtained as a result of measurements, which is converted to the specific sensitivity of the coating using the following formula

$$\eta = \frac{\Sigma E}{\Phi_0 \cdot S \cdot \tau} \cdot \frac{e}{\varepsilon} = K \cdot \frac{e}{\varepsilon} \qquad (3)$$

where $\Sigma E$ is the total energy yield of the radiator coating, eV; $K$ is the specific energy yield of the radiator coating, MeV/neutron; $\varepsilon$ is the ionization energy of the IC working gas (argon), 30 eV; $e$ is the electron charge, C; $\Phi_0$ is the neutron flux, cm$^{-2} \cdot$s$^{-1}$; $S$ is the electrode area, cm$^2$; $\tau$ is the spectrum recording time, s; and $\eta$ is the specific sensitivity of the radiator coating, C/neutron.

Fig. 4 presents the output pulse spectra for the lithium-containing functional layer of the composite radiator coating and the industrial boron radiator coating for the KNK-53 chamber. Spectrum 1 (see Fig. 4) includes a distinctly observable peak in the 2.75 MeV region corresponding to tritium, and a broad peak with an energy below 2.05 MeV related to the alpha particle. The peaks have a broad shape due to partial energy losses in the radiator material. The energy yield of the coating when irradiated with thermal neutrons was 3.7 10$^{-3}$ MeV/neutron. The specific neutron sensitivity of the lithium-containing composite radiator coating was $\eta = 2.0 \cdot 10^{-17}$ C/neutron.
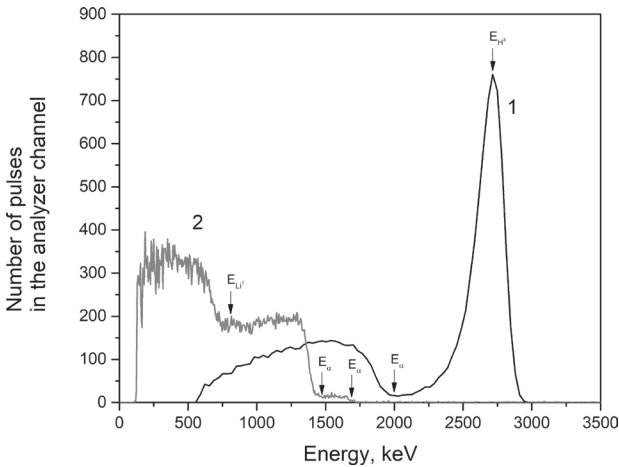
Spectrum 2 (see Fig. 4) includes visible broad bands



**Figure 4.** Spectrum of output pulses from charged particles for electrode samples: 1 – with a lithium-containing radiator coating; 2 – with a boron radiator coating for the KNK-53 chamber.

with energies of less than 0.83 MeV (due to the presence of $^7$Li), as well as with energies of 1.47 and 1.7 MeV (owing to the alpha particle). The energy yield of the coating when irradiated with thermal neutrons was 0.9·10$^{-3}$ MeV/neutron. The specific neutron sensitivity value of the boron coating was $\eta = 5.0 \cdot 10^{-18}$ C/neutron.

The sensitivity of the lithium-containing radiator coating is 4.0 times higher, and the energy yield is 4.1 times higher. The values of the ratios are generally comparable, and the slight difference is explained by different geometric characteristics of the electrodes.

A sample of the lithium-containing radiator coating was tested thermocyclically. Annealing conditions for a single cycle: inert medium – argon (absolute pressure 10$^5$ Pa); annealing temperature – 600 °C; exposure time – 4h; heating rate – 5°/min; inertial cooling. The results of determining the specific neutron sensitivity of the coating in the thermocyclic test process are shown in Table 1.

It follows from the above data that the initial annealing is followed by a decrease in sensitivity due to the thermal emission of a portion of the fluoride-lithium coating. The specific neutron sensitivity, energy yield and radiation coating surface density values are constant with a confidence probability of $p = 0.95$. Following the decrease in the value in the course of thethermocyclic loads, the specific neutron sensitivity of the functional layer is 1.5·10$^{-17}$ C/neutron on the average. The specific neutron sensitivity value of the boron radiator coating for the KNK-53 chamber in conditions of similar thermocyclic tests decreases from 5.0·10$^{-18}$ to 1.0·10$^{-18}$ C/neutron, which is lower than the lithium-containing coating characteristics.

**Table 1.** Dynamics of changes in the characteristics of the lithium-containing coating functional layer in the thermocyclic test process

| Thermocyclic loads | Specific neutron sensitivity η, C/neutron | Specific energy yield, MeV/neutron | Surface density of functional layer, mgm/cm$^2$ |
|---|---|---|---|
| Prior to annealing | 2,0·10$^{-17}$ | 3,7·10$^{-3}$ | 2,5 |
| Annealing 1 | 1,5·10$^{-17}$ | 2,8·10$^{-3}$ | 1,8 |
| Annealing 2 | 1,5·10$^{-17}$ | 2,8·10$^{-3}$ | 1,8 |
| Annealing 3 | 1,5·10$^{-17}$ | 2,8·10$^{-3}$ | 1,8 |
| Annealing 4 | 1,5·10$^{-17}$ | 2,8·10$^{-3}$ | 1,8 |

# Lithium-containing radiator coated IC

An IC model was developed and manufactured (Fig. 5) based on the data obtained. The chamber consists of two parallel plates (electrode profiles), each of which had four earlier tested electrode samples with a lithium-containing composite radiator coating applied to it. The electrode profiles are contained in a cylindrical case with a diameter of 50 mm, and the gap between the electrodes is 3 mm. Since the radiator material (lithium fluoride) is a dielectric, a metal mesh of a wire with a diameter of about 180 μm is attached to the surface of the electrode plates for the current collection (Fig. 6). The chamber is filled with theworking gas (argon) with an absolute pressure of 1.2·10$^5$ Pa.

The IC model was tested on a dedicated test bench being irradiated with a neutron flux of 6·10$^3$ cm$^{-2} \cdot$s$^{-1}$ from a Pu-Be source. Measurements were undertaken in the current mode using a KVVS controller from the Avtotest APK suite. The measured current value is about 5·10$^{-12}$ A.
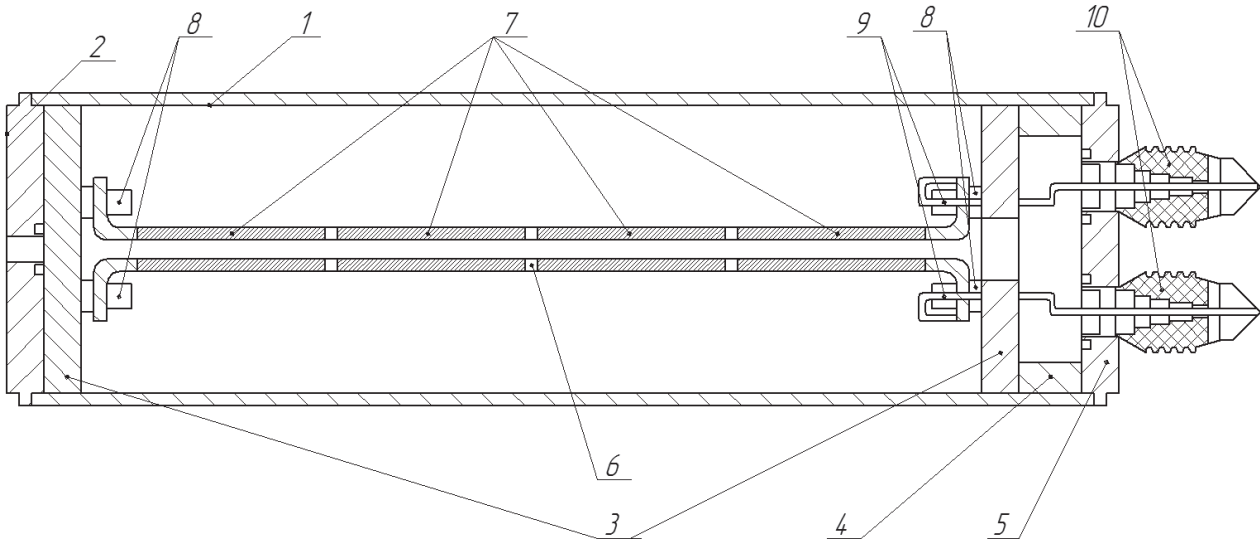
**Figure 5.** IC model: 1 – body; 2 – flange; 3 – guide disc; 4 – O-ring; 5 – flange with electrode leads; 6 – electrode profile with a mesh; 7 – electrodes with lithium-containing radiator coating; 8 – support insulators; 9 –electrode contact leads; 10 – electrical insulators.
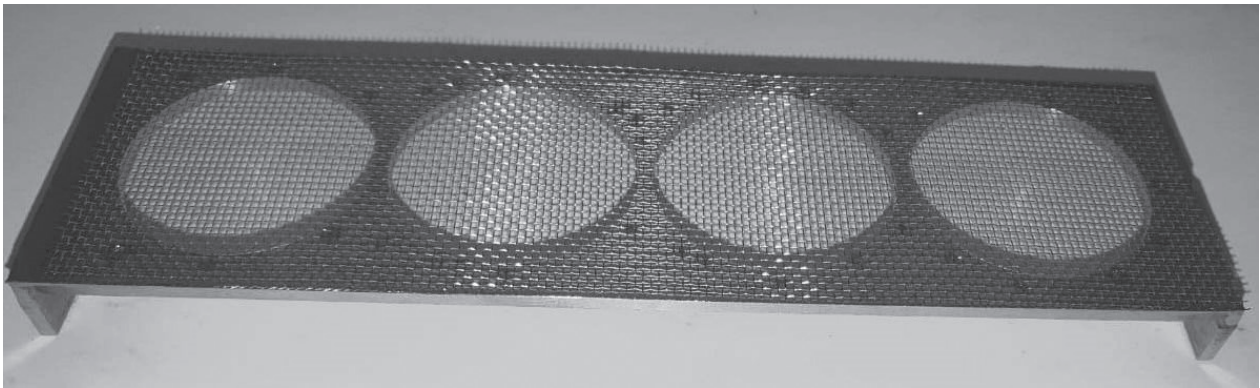


**Figure 6.** Electrode profile with a mesh.

The volt-ampere characteristic (VAC) of the model is shown in Fig. 7. The VAC slope at a voltage of $U \geq 300V$ is $s = 0.02\%/V$, which corresponds to the non-linearity of the loading characteristic, $\theta$, of not more than 3.8%. The deviation from the linearity of the loading characteristic $\theta$ is determined by equation (Dmitriev, Malyshev 1975):

$$\theta = \frac{U \cdot s}{2 + 10^{-2} \cdot U \cdot s} \qquad (4)$$

With a total radiator coating area of 56.5 cm², the measured sensitivity of the IC model was $0.8 \cdot 10^{-15}$ A·s·cm²/neutron, which agrees with the design value of $1.0 \cdot 10^{-15}$ A·s·cm²/neutron.

The composite lithium-containing coating has shown to be serviceable in the IC model design, which indicates that there is a high potential for using the proposed radiator material in neutron flux detection devices.



**Figure 7.** Volt-ampere characteristic of an IC model with a lithium-containing radiator coating.

## Conclusions

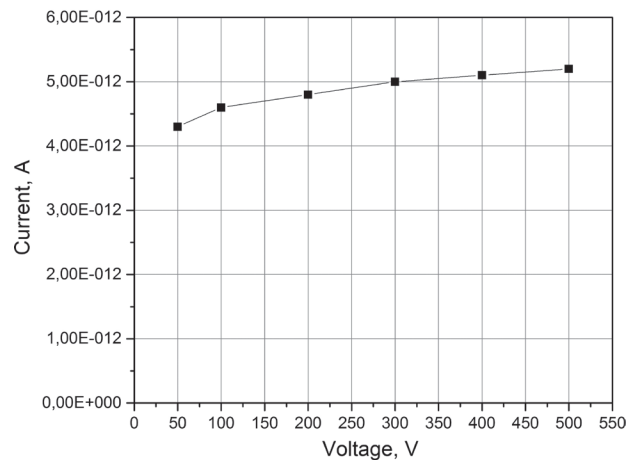The paper presents the results of investigating a radiator lithium-containing coating with a composite two-layer microscale structure that consists of an intermediate silicate layer and a fluoride-lithium functional neutron-sensitive layer of a given thickness (10 to 20 µm). An examination of the microstructure and phase composition of the coating components has shown that the basis for the intermediate adhesive layer is formed by alphaquartz and clay mineral (kaolinite).

The adhesion of the functional lithium fluoride layer is achieved due to the forces caused by the developed surface of the intermediate silicate layer. It has been found that the coating remains intact after vibration tests at a low-frequency resonant impact of up to 35 Hz and at a high-frequency impact of up to 200 Hz.

Radiometric characteristics of the lithium-containing radiator coating were studied. The specific neutron sensitivity was $\eta = 2.0 \cdot 10^{-17}$ C/neutron. This value is four times higher than that for the boron radiator coating of the industrial KNK-53 IC. It has been found that thermocyclic tests at 600 °C after the initial annealing cause the specific sensitivity to decrease by a factor of about 1.5 due to the partial heat emission of the lithium-containing layer. The value of the specific neutron sensitivity stabilizes in the course of subsequent thermal cycles and remains constant (about $1.5 \cdot 10^{-17}$ C/neutron).

It is for the first time that possibilities have been demonstrated for using the $^6$Li isotope as a component of the IC radiator coating for the neutron flux detection sensors. Results are presented from neutronic studies of the lithium-containing radiator coating as part of the developed IC model. The measured value of the IC model current was $5 \cdot 10^{-12}$ A, the neutron flux from the Pu-Be source being $F = 6 \cdot 10^3$ cm$^{-2} \cdot$s$^{-1}$. The sensitivity of the chamber model was about $10^{-15}$ A$\cdot$s$\cdot$cm$^2$/neutron. The volt-ampere characteristic slope for the chamber model with a lithium-containing radiator coating was 0.02%/V at a voltage of over 300 V.

Further studies will be aimed at improving the IC model's design features and determining its pulse characteristics, and conducting durability tests to increase the sensitivity and stability of the lithium-containing radiator coating's characteristics in the course of thermal cyclic testing.

# References

- Allen VD (1962) Neutron registration. Moscow. Gosatomizdat Publ., 196 pp. [in Russian]
- Baskov PB, Marichev GV, Sakharov VV, Stepanov VA (2022) Nuclear-optical converters for detecting intense neutron. Nuclear Energy and Technology 8(1): 31–36. https://doi.org/10.3897/nucet.8.82558
- Baskov PB, Mosyagina IV, Sakharov VV, Ivkina OV, Khudin AS, Kirichenko GP (2018) Small thorium fission chambers for recording fast neutrons in reactor installations. AtomicEnergy 125(1): 33–38. https://doi.org/10.1007/s10512-018-0438-x
- Bolozdynya AI (2017) Experimental nuclear physics. Lecture No. 2. Interaction of charged particles with matter. https://enpl.mephi.ru/download/lectures/lect_5.pdf [accessed Nov. 29, 2023] [in Russian]
- Dmitriev AB, Malyshev EK (1975) Neutron ionization chambers for reactor equipment. Moscow, Atomizdat Publ., 96 pp. [in Russian]
- Egorov AV, Baskov PB, Sakharov VV, Mosyagina IV (2015) Uranium oxide radiator of the fission ionization chamber. Patent RF, No. 152036. https://elibrary.ru/download/elibrary_38370451_98101785.pdf [accessed Nov. 1, 2023] [in Russian]
- Experimental nuclear physics. Volume 1 (1955) (Edit. E. Segre). Moscow, Foreign Literature Publ., 1840 pp. [in Russian]
- Glazyuk YaV, Dmitriev AB, Fedoseev VA (2017) High-temperature ionization fission chamber for control and protection systems of nuclear installations.Patent RF, No. 2630260. https://elibrary.ru/download/elibrary_38286699_38973367.pdf [accessed Nov. 1, 2023] [in Russian]
- GOST 29075-91 (2004) Nuclear instrumentation systems for nuclear power plants. Moscow, IPK House of Standards Publ., 22 pp. https://ohranatruda.ru/upload/iblock/6dd/4294825607.pdf [accessed Nov. 29, 2023] [in Russian]
- Mosset JB, Stoykov A, Greuter U, Hildebrandt M, Schlumpf N, Van Swygenhoven H (2014) Evaluation of two thermal neutron detection units consisting of ZnS/$^6$LiF scintillating layers with embedded WLS fibers read out with a SiPM. Nuclear Instruments and Methods 764: 299–304. https://doi.org/10.1016/j.nima.2014.07.060
- Nakamoto K (1966) Infrared spectra of inorganic and coordination compounds. Moscow, Mir Publ., 411 pp. [in Russian]
- Osovizky A, Pritchard K, Ziegler J, Binkley E, Yehuda-Zada Y, Tsai P, Thompson A, Cooksey C, Siebein K, Hadad N, Jackson M, Hurlbut C, Ibberson R, Baltic GM, Majkrzak CF, Maliszewskyj NC (2018) $^6$LiF:ZnS(Ag) Mixture Optimization for a Highly Efficient Ultrathin Cold Neutron Detector. IEEE Transactions on Nuclear Science 65(4): 1025–1032. https://doi.org/10.1109/TNS.2018.2809567
- Papko LF, Kravchuk AP (2013) Physico-chemical methods of research of inorganic substances and materials. Minsk, BSTU Publ., 100 pp. [in Russian]
- Plyusnina II (1977) Infrared spectra of minerals. Moscow, Moscow State University Publ., 174 pp. [in Russian]
- Sakharov VV, Baskov PB, Berikashvili VSh, Ivkina OV, Kosov DE, Mosyagina IV, Frolov NN, Sharipova MA (2012a) Oxide nanolevel modification of the surface of inorganic materials. Rossijskij Himicheskij Zhurnal 1–2: 36–43. https://elibrary.ru/download/elibrary_18013627_10974709.pdf [accessed Nov. 1, 2023] [in Russian]
- Sakharov VV, Baskov PB, Mosyagina IV, Frolov NN, Kurbatkin II, Muravyeva TI, Torskaya EV, Ivkina OV, Sharipova MA (2012b) Chemical synthesis of neutron-detecting ultrathin optical materials. Izvestiya vuzov. Yadernaya Energetika 4: 130–142. https://doi.org/10.26583/npe.2012.4.15 [in Russian]
- Shulgin BV, Petrov VL, Pustovarov VA, Arbuzov VI, Raikov DV, Ivanovskikh KV, Ishchenko AV (2005) Scintillation neutron detectors based on $^6$Li-silicate glass activated by cerium. Fizika tverdogo tela 8: 1364–1367. https://journals.ioffe.ru/articles/viewPDF/3910 [accessed Nov. 5, 2023] [in Russian]
- Subbotin VI, Arnoldov MN, Ivanovsky MN, Mosin AA, Tarbov AA (1999) Lithium. Moscow, IzdAT Publ., 1999, 263 pp. [in Russian]
- Voytovetsky VK, Tolmacheva NS (1959) Lithium-silicate scintillation glasses for detecting slow neutrons. Atomnaya energiya 4: 472–475. https://elib.biblioatom.ru/text/atomnaya-energiya_t6-4_1959/p472/ [accessed Nov. 5, 2023] [in Russian]
- Voytovetsky VK, Tolmacheva NS (1961) Scintillation glasses with increased light output for neutron detection. Atomnaya energiya 5: 504. https://elib.biblioatom.ru/text/atomnaya-energiya_t10-5_1961/p504/ [accessed Nov. 5, 2023] [in Russian]